

Supercapacitor Energy Storage for Wind Energy Applications

Chad Abbey, *Student Member, IEEE*, and Géza Joos, *Fellow, IEEE*

Abstract—As wind energy reaches higher penetration levels, there is a greater need to manage intermittency associated with the individual wind turbine generators. This paper considers the integration of a *short-term* energy storage device in a doubly fed induction generator design in order to smooth the fast wind-induced power variations. This storage device can also be used to reinforce the dc bus during transients, thereby enhancing its low-voltage ride through (LVRT) capability. The topology is evaluated in terms of its ability to improve the performance both during normal operation and during transients. Results show that when storage is sized based upon the LVRT requirement, it can effectively damp short-term power oscillations, and it provides superior transient performance when compared with conventional topologies.

Index Terms—Doubly fed induction generator (DFIG), energy storage, power quality, supercapacitors, wind energy.

NOMENCLATURE

b_i	Degree of fulfillment for the i th rule.
c_i	Consequent for the i th rule.
C_{ess}	Equivalent capacitance of the supercapacitor bank.
E_{ess}	Energy of the energy storage device.
E_{LVRT}	Base energy, which is defined by the area above the low-voltage ride through (LVRT).
P_{conv}	Grid-side converter real power.
P_{ess}	Power delivered to the storage device.
P_{grid}	Wind power delivered to the grid from the wind turbine generator (WTG).
$P_{\text{grid,ref}}$	Wind power reference.
$\Delta P_{\text{grid,ref}}$	Change in the wind power reference due to storage limits.
ΔP_{pred}	Change in the wind power due to prediction errors.
P_s	Stator power.
$V_{\text{dc,ref}}$	DC voltage reference.
V_{pcc}	Voltage at the point of connection.
β	Pitch angle.
ω_m	Mechanical angular speed.

Paper IPCSD-06-112, presented at the 2005 Industry Applications Society Annual Meeting, Hong Kong, October 2–6, and approved for publication in the IEEE TRANSACTIONS ON INDUSTRY APPLICATIONS by the Industrial Power Converter Committee of the IEEE Industry Applications Society. Manuscript submitted for review July 26, 2005 and released for publication December 29, 2007. This work was supported in part by the National Science and Engineering Research Council of Canada and in part by Natural Resources of Canada.

The authors are with the Department of Electrical and Computer Engineering, McGill University, Montréal, QC H3A 2A7, Canada (e-mail: chad.abbey@mail.mcgill.ca; geza.joos@mcgill.ca).

Digital Object Identifier 10.1109/TIA.2007.895768

I. INTRODUCTION

WHILE wind energy continues to grow worldwide, the industry will need to confront the challenges associated with higher levels of penetration. At the point where wind represents a significant component of the generation mix, all of its shortcomings will be amplified. In anticipation of new wind projects and based upon experience gained worldwide, most utilities have developed or revised existing grid codes in order to address the potential problems posed by high wind penetration levels [1].

For new wind farms, the types of interconnection studies that are required at the distribution level can be summarized in terms of power quality and voltage impacts (short term and long term). For bulk systems, the typical concerns are more related to the impact on stability, voltage support, and ability to balance the intermittency using complementary generation, typically by allocating sufficient spinning reserves. Various studies have been completed in these areas, [2]–[4]; however, further work is still required in order to provide a generalized methodology, as existing methods are either not yet sufficient, or have not been made public.

This paper presents a WTG with energy storage and the associated storage management algorithm. A thorough evaluation of the performance of the system is performed using a variety of test conditions, considering various sizes of storage, different wind characteristics, and power predictions. System characteristics under normal operation, as well as the ability of storage to improve the transient performance of the WTG, were considered.

II. WIND ENERGY AND STORAGE

Complementing wind with storage has been considered in various cases [4]–[8] but has yet to be adopted by the industry, primarily due to the cost. In order to justify the associated expense, the storage device will need to provide a marketable improvement in the overall performance of the generator. In addition, the improved performance must be mandated by utilities through the interconnection requirement; otherwise, the motivation to add additional equipment is nonexistent. That said, storage can offer improvements in both power control and management of energy during disturbances, e.g., short circuits.

A. Dispatchable Power

Although grid codes have not explicitly stated the need for firm power control for wind farms, the trend points in that direction. A reduction of the *short-term* power variations of a WTG

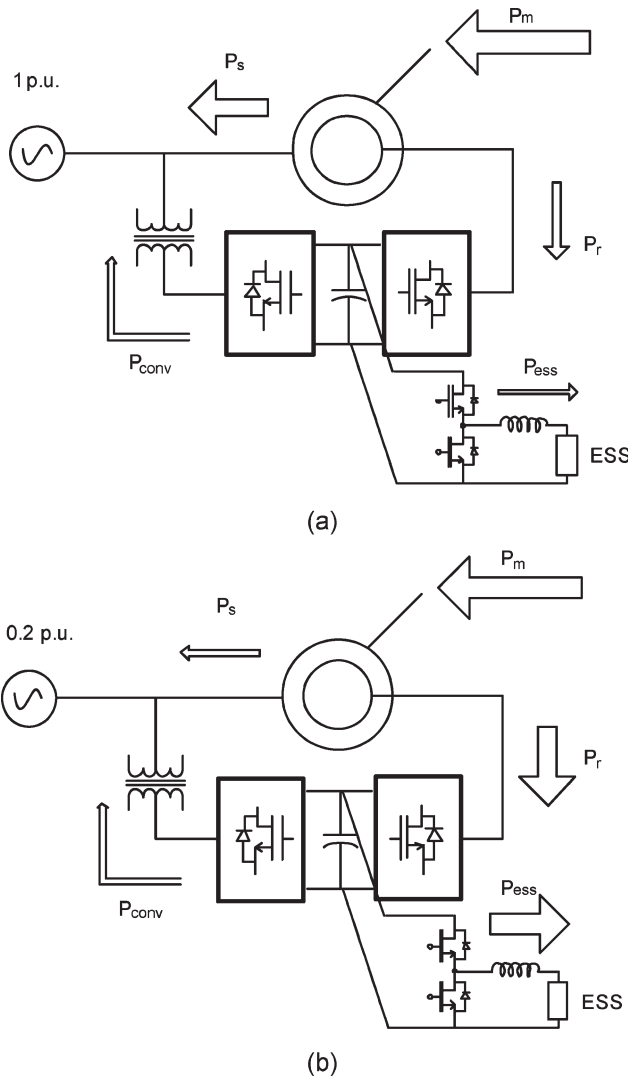


Fig. 1. Energy flow diagram in the DFIG during (a) normal operation and (b) low-voltage conditions.

can be realized in essentially two ways: 1) through storage or 2) by using a variable-speed generator that operates at suboptimal power points, as described in [5]. Although storage comes at a greater cost, it possesses a number of advantages: it can be accessed at any operating condition, the operation of the machine need not be modified, and it can also enhance LVRT, potentially resulting in transient stability improvements.

B. Doubly Fed Induction Generator (DFIG)–Energy Storage System (ESS)

Energy storage devices can be readily integrated into the design of the DFIG using a bidirectional dc/dc converter coupled with the dc bus (Fig. 1). For this topology, either the line-side converter or the storage converter controls the dc bus voltage, whereas the other is responsible for regulating the storage power. Fig. 1(a) shows the flow of energy for operation at a supersynchronous speed—power flows from the rotor windings to the converter. For this case, some energy is stored while the remainder is exported onto the grid via the line-side converter. Similar diagrams can be developed for subsynchronous operation and storage discharging.

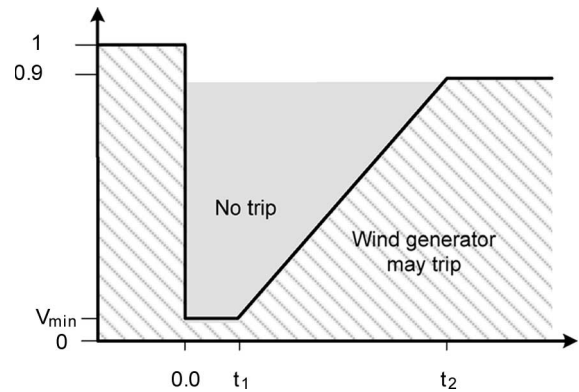


Fig. 2. Typical LVRT characteristics.

C. Energy Management Under Faults

LVRT characteristics have been developed, e.g., [9], which dictates the voltage profile for which a WTG must remain connected to the system (Fig. 2). In order to be able to meet this requirement, the control system and the hardware has to be modified to manage the energy produced by the WTG during the low-voltage event. Without energy management, the power produced by the WTG under fault conditions will remain within the electric machine, resulting in an increased mechanical speed.

A certain amount of energy can be stored in rotating masses; however, this is finite due to the maximum allowable rotor operating speed. Furthermore, it is preferable to keep the speed constant at the prefault value, in order to minimize transients upon reclosing or reestablishment of the system connection.

Options available to handle the energy that the grid cannot absorb are listed as follows:

- 1) dumping the energy in a resistor, which is typically connected to the dc bus, regulating the dc bus to within $\pm 10\%$ of its nominal value;
- 2) shorting the rotor windings through a resistor and operating the machine as a conventional induction machine;
- 3) dumping the energy in an electrical storage device, for example, supercapacitor, superconducting magnetic energy storage, and batteries.

In the latter case, the storage device must be sized to absorb the energy produced under the worst conditions—a three-phase fault, lasting for the duration specified in the LVRT curve, i.e., t_1 in Fig. 2. The approximate required energy storage capability is then given by $E = V \cdot t_1 = t_1$ per unit (p.u.). For a more precise sizing, the entire area above the curve should be considered, as given in (2).

The WTG needs to remain connected during the disturbance to help limit the impact at the local bus and aid in the recovery of the voltage to the nominal range after the disturbance is isolated by the system protection. This is accomplished by supplying a fixed reactive power, or alternatively by actively regulating the system voltage. Even more important, the generator supplies energy as soon as the fault is cleared, without requiring it to be restarted. Energy storage can aid in both these processes by holding the dc voltage during the fault and limiting the

TABLE I
PROPERTIES OF SHORT-TERM STORAGE TECHNOLOGIES
AND A LEAD ACID BATTERY

Technology	Energy Cost (\$/kWh/year)	Power Cost (\$/kW/year)	Time Scale	Round Trip Efficiency
Lead Acid	69	91	60–300 min	63%
High Speed Flywheel	96	1.2	0.006–6 min	89%
Super Capacitor	711	6	0.006–6 min	86%
SMES	370000	59	0.006–0.06 min	21%

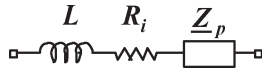


Fig. 3. Dynamic model for a supercapacitor.

acceleration of the machine, avoiding the disconnection of the wind park and supporting the recovery of the system following the event.

D. Supercapacitors

For *short-term* power exchange, the most commonly implemented technologies are presented in Table I, along with the characteristics in terms of cost, time scale, and efficiency, based upon information presented in [7]. The case of lead acid batteries is given as a point of reference. The two most promising *short-term* storage devices—flywheels and supercapacitors—both offer similar characteristics and are both suitable for wind energy applications.

In this paper, supercapacitors were considered, as they represent a storage device that has a high energy density and presents a good efficiency. In addition, they have a much higher life cycle than batteries.

1) *Models*: Various models can be used for supercapacitors. Depending on the type of study, more or less detail may be required. Very accurate models, based upon the equivalent circuit given in Fig. 3 have shown to provide very good agreement when compared with experimental results [10]. This modeling is valid over the entire frequency spectrum, where the frequency-dependent part of the model is given by

$$Z_p(j\omega) = \frac{\tau \cdot \coth(\sqrt{j\omega\tau})}{C \cdot \sqrt{j\omega\tau}}. \quad (1)$$

The four parameters need to be obtained from measurements of the device. For the purpose of this study, the characteristics of the device in the low-frequency range of the spectrum were considered, which reduces to essentially a large capacitance in series with its ESR. This choice was based on the need to focus more on energy flow as opposed to efficiency and switching transients.

2) *Supercapacitor Sizing*: Here, the base energy for the supercapacitors was chosen such that it would be capable of storing the full rating of the system during the entire low-voltage condition, as given by the LVRT requirement in [9].

The requirements of the energy storage device E_{LVRT} can be calculated as the area above the LVRT curve and below 0.9 p.u. line, i.e.,

$$E_{LVRT} = P_{base} \{(0.9 - V_{min})t_1 + 0.5(t_2 - t_1)(0.9 - V_{min})\} \quad (2)$$

where V_{min} , t_1 , and t_2 describe the LVRT profile.¹ This defines the amount of energy that must be managed during the fault. Assuming that the maximum voltage across the device was equal to $V_{dc,ref}$, the required value of the capacitance is found using

$$C_{ess} = \frac{2E_{LVRT}}{V_{dc,ref}^2}. \quad (3)$$

III. ENERGY STORAGE SCHEDULING

For the DFIG–ESS, the dc voltage control handles the chopper circuit, whereas the primary function of the supply-side converter becomes the regulation of the power supplied to the grid, through the reference value, $P_{grid,ref}$. Details of the converter control can be found in [11]. Details regarding scheduling of the energy to and from the storage device are presented here.

A. Storage Management

In its simplest form, the power of the combined DFIG and ESS system is dispatched in order to supply a set amount of power. However, this assumes that the state of operation of the generator is always relatively near that of the set point and neglects the current limitations of the different converters. Furthermore, in certain cases, the storage device may not be used effectively, particularly when there is a large mismatch between the set point power and the output of the machine. For a wind generator, the operating point is constantly varying since the energy source is dependent on the local environmental conditions. By allowing the set point to vary, the time scale over which the storage device can be applied is extended, thereby maximizing the benefits of the storage, while relinquishing only slightly the firm regulation of the output power. Through a proper design of the management system, the storage device can be kept in operation by curtailing or boosting the power reference, near the upper or lower storage limits.

However, setting the power reference in order to ensure that the ESS remains in operation is difficult since it is not known exactly how it should vary. Wind prediction algorithms, although constantly being improved, are still prone to inaccuracies. Furthermore, the relationship to the output power is not always precisely known. The need to cover normal operation, limiting conditions, as well as transient behavior of the system makes this control challenging.

Fuzzy-rule-based systems have been shown to be effective in various power system problems, e.g., [12], and are well suited

¹A design example for typical WTG and LVRT profile can be found in the Appendix.

TABLE II
RULE BASE FOR THE STORAGE MANAGEMENT SCHEME

Rule		c_i
1	If E_{ess} is small then ΔP_{grid} negative large.	0.5
2	If E_{ess} is small-medium then ΔP_{grid} negative small.	0.1
3	If E_{ess} is medium then ΔP_{grid} is zero.	0
4	If E_{ess} is medium-big then ΔP_{grid} positive small.	0.1
5	If E_{ess} is big then ΔP_{grid} positive large.	0.5
6	If V_{pcc} is small then ΔP_{grid} positive small.	0.2
7	If V_{pcc} small then β large.	1

to the present system. Using the predicted wind power production, energy storage device status and history, and ac voltage measurements, a fuzzy-based energy management system can be used to set the power level in order to optimize the overall operation of the system.

The rule base was developed in order to attempt to balance the needs to smooth the output fluctuations, secure sufficient reserves for contingencies, and ensure that the storage device remains in operation at all times (Table II). The initial set point is determined using the predicted wind power production, which is assumed to be have been provided from hour-ahead forecasts. This reference value is then modified by the algorithm to ensure that there is always some base amount of energy stored in the device, and likewise that there is always a certain threshold below the upper limit. The membership functions for the E_{ess} and V were varied using a process of trial and error (Fig. 4). The widths of the functions were adjusted until a desirable response was achieved, one that made good use of the storage capacity and respected the margin required for transients.

For the transient component of the control, a number of variations were studied using the measured voltage magnitude. In the event of a voltage sag, various changes to the reference power were attempted—increase, decrease, or no change. Ultimately, the most effective signal proved to be to boost the power reference slightly upon initiation of a fault, although the improvement was marginal. The pitch angle β was also increased in proportion to the membership function in order to limit the input torque during voltage sags. Together, the normal and transient functions of the management system were designed to help smooth the output power, ensure that the storage device remains in operation, and limit the acceleration of the generator during disturbances.

Inference and aggregation of the rules was used in order to produce the final value for the reference power, i.e., a value between 0 and 1, which is then converted to a reference value using the base power. The weighting of the various rules is most easily represented by

$$\Delta P_{\text{grid,ref}} = \frac{\sum_{i=1}^K b_i c_i}{\sum_{i=1}^K b_i} \quad (4)$$

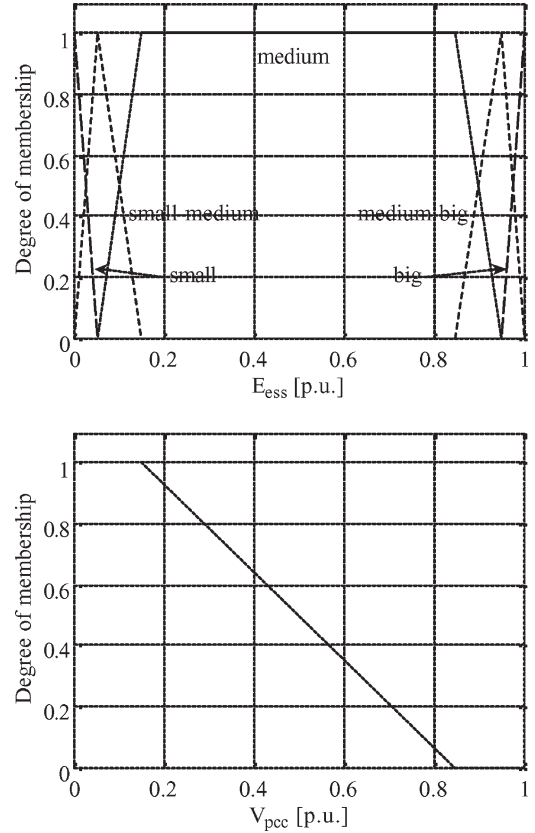


Fig. 4. Membership functions for stored energy E_{ess} and the voltage at the PCC V_{pcc} .

where K is the number of rules, and b_i and c_i are the degree of fulfillment and consequent of the i th rule, respectively. The consequents for each of the rules have been included in Table II. The values for rules 1 and 2 are negative, which makes $\Delta P_{\text{grid,ref}}$ also negative, resulting in a decrease in $P_{\text{grid,ref}}$.

In order to account for possible errors in the prediction algorithm, the integral of the difference between the actual storage level E_{ess} and the nominal storage level E_{nom} was used, i.e.,

$$\Delta P_{\text{pred}} = \frac{1}{T_{\text{ess}}} \int (E_{\text{ess}}(t) - E_{\text{nom}}) dt \quad (5)$$

where T_{ess} is the time constant associated with the duration of the storage, which was chosen as 25 s (the window of the simulation). The final reference power $P_{\text{grid,ref}}$ that is used to schedule the system output power is obtained from the sum of the change in the reference value, as determined by the management algorithm, the integral term (5), and the WTG power as calculated from the predicted wind speed. That is

$$P_{\text{grid,ref}} = P_{\text{grid,pred}} + \Delta P_{\text{grid}} + \Delta P_{\text{pred}} \quad (6)$$

As β is a result of only one rule, it simply has the effect of increasing the pitch angle during a low-voltage event, which helps to limit the input torque during a local system fault. However, there is a relatively large mechanical time constant associated

with this signal (0.1–0.5 s), and therefore, its ability to improve the response during very short fault durations is limited.

IV. SYSTEM CHARACTERISTICS

Here, the operation of the system was demonstrated using a number of different scenarios in order to illustrate the effectiveness of the storage management scheme under both transient and normal conditions. Furthermore, the operation was considered for different storage levels and for cases where the wind power prediction was less than ideal. The results are discussed throughout, and the general advantages as well as limitations of this strategy are highlighted.

A. Normal Operation

First, the operation of the system under typical conditions is considered; under typical wind speeds, the storage algorithm is used to smooth out the short-term variations in wind power (Fig. 5). As can be noted from Fig. 5, the supply-side converter exchanges power with the system in order to account for *short-term* variations in the stator power P_s that are either above or below the reference power. This is reflected in the level of energy in the storage device, which increases as power is delivered to the system and decreases as it is absorbed. For completeness, the storage voltage and charging current are included.²

B. Parameter Dependence

As the performance of the management strategy depends largely on the rating of the storage device, as well as the accuracy of the estimate of wind power, the effect of these two variables on the performance of the system is considered. Although the area under the LVRT was used as the base value for rating the storage device, it is possible that similar gains can be realized with a reduced value. Furthermore, the accuracy of the prediction algorithm tends to vary greatly, and while these technologies are being improved, the management scheme should still be able to provide benefits even under nonideal cases.

1) *Storage Rating*: The effect of the rating of the storage device was considered by subjecting the system with different storage ratings to the wind profile in Fig. 6(a). Here, the base case (1 p.u.) is defined by the LVRT. In addition, the results were contrasted with the case of no storage, where the generator is operating with maximum power point tracking (MPPT). The integral term was not included here, in order to isolate the effect of the storage level. The case of 1 p.u. is able to maintain a constant output power throughout, whereas the two other cases show greater variations when the output power is greater than or less than the average power for extended periods of time (Fig. 6). This is reflected in the change in the storage level, which approaches the upper and lower limits for the cases of 0.5 and 0.2 p.u.

2) *Wind Power Prediction Accuracy*: As modern wind power prediction methods do not always accurately estimate

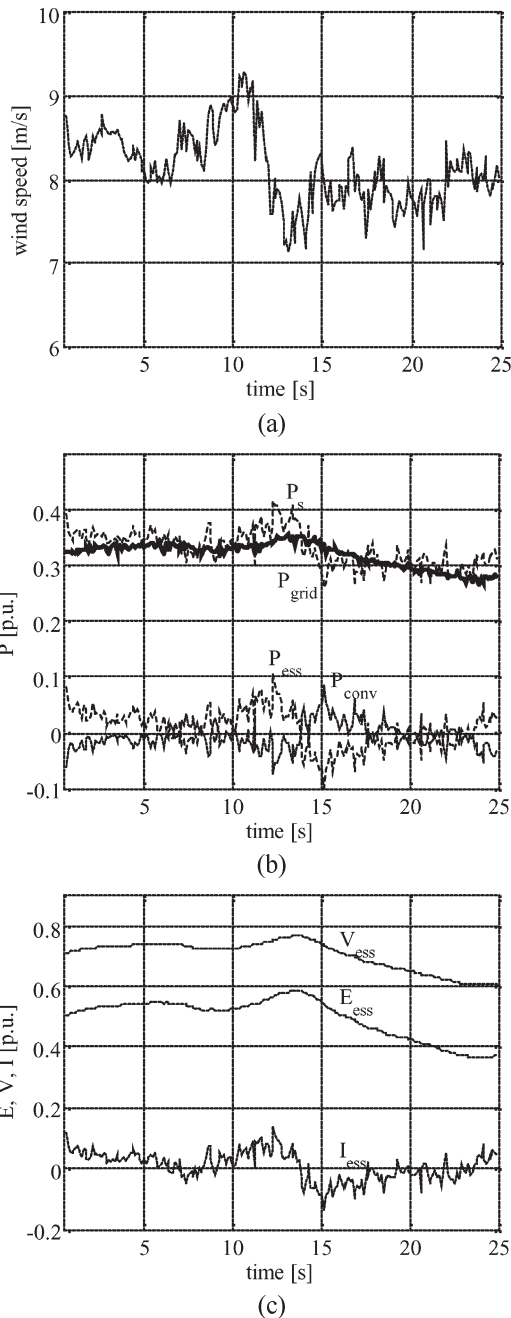


Fig. 5. Operation of the system under typical wind conditions: (a) wind speed; (b) real power delivered to the grid, P_{grid} , from the machine stator, P_s , from the line-side converter, P_{conv} , and to the storage device, P_{ess} ; and (c) storage level E_{ess} , voltage V_{ess} , and charging current I_{ess} .

the power production, it is important to understand the effect of erroneous P_{pred} . This was done using different wind conditions for a given P_{pred} . In the first case, the predicted power matches the actual power. Two other cases were considered where the wind speeds were scaled in such a way that it resulted in output powers that were 0.1 and 0.2 p.u. higher than the predicted value (Fig. 7). The algorithm corrects for this in two ways: first, through the storage level terms, and second, through the integral term. Although in the first case the system is able to smooth the output power, in cases with prediction errors, the output power reference is shifted to the new set points with varying degrees of success.

²Base values are provided in the Appendix.

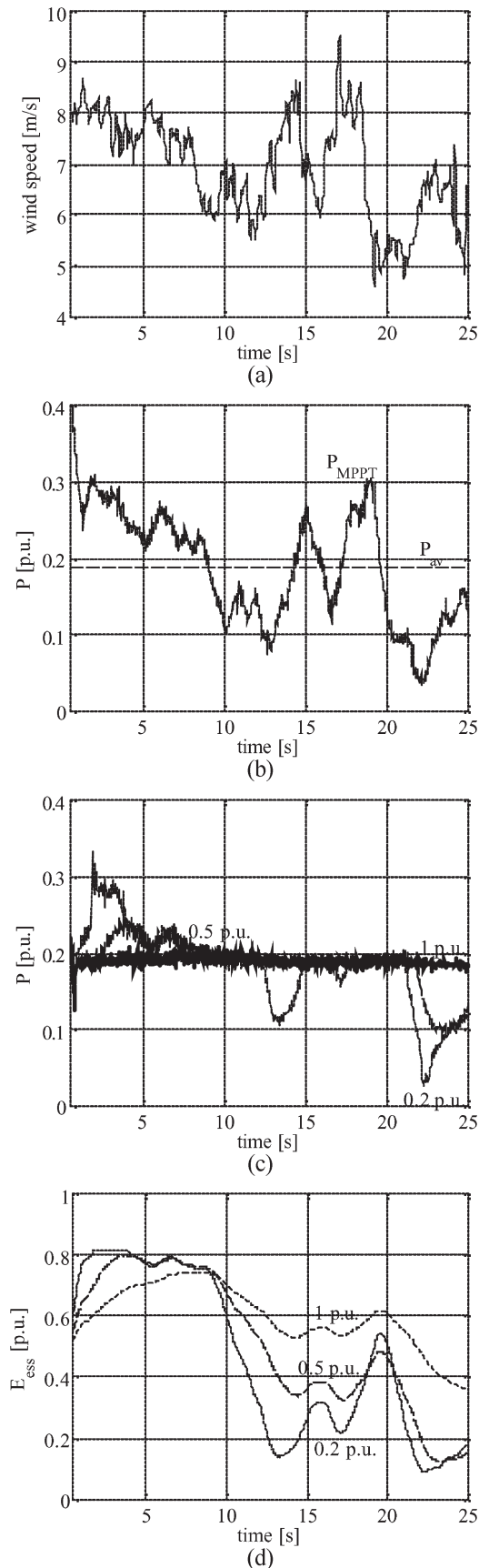


Fig. 6. Performance for different storage ratings. (a) Wind profile. (b) DFIG operating with MPPT. (c) Output powers for storage ratings of 1, 0.5, and 0.2 p.u. (d) Corresponding storage level.

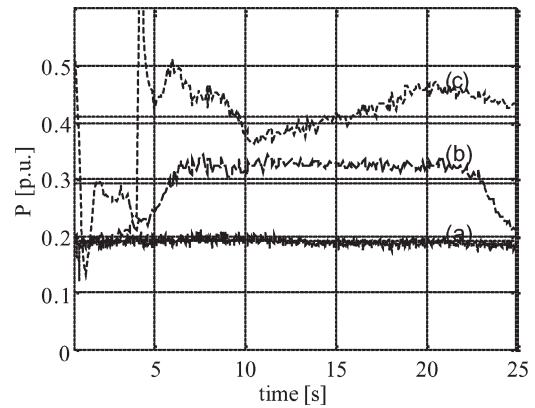


Fig. 7. Variation of output power for different errors in predicted output power: (a) no error; (b) 0.1 p.u. error; and (c) 0.2 p.u. error.

If the case of 0.1 p.u. is considered, it can be noted that the reference power adjusts up to near the new average value. The variation in the output power is small, and it ramps down near the end of the test interval due to the time constant associated with the integral term. In the more extreme case, there is a large transient as the reference value is shifted to account for the error in prediction. Initially, the original reference point—which is based upon the wind power prediction—is achieved by storing large amounts of energy. This quickly results in a shift to the new reference value, which accounts for the spike. However, beyond 5 s, the system is able to supply a relatively constant output albeit with greater fluctuations than the first case.

A number of important remarks can be made at this point. First, the storage management scheme can be designed in order to readjust the power reference for prediction errors and continues to smooth the output power. This shift in the operating point makes better use of the storage since it is operated about its nominal state of charge.

Second, in a larger picture, this may or may not be desirable as it fails to circumvent the problem associated with inaccurate power estimates—there is still an overall surplus (or short fall) in generation, and therefore, other sources must be curtailed (ramped up). Of course, this will depend, in a large part, on the relative installed capacity. Therefore, although *short-term* storage can be effectively used to solve power quality issues associated with wind, only long-term storage, and likely a combination of *short-* and *long-term* storage, will be able to properly address the scheduling problem associated with prediction errors.

Finally, for larger prediction errors, a correspondingly larger storage rating is required to retain the same performance as without error. This is true for both the energy and power rating of the device. This reinforces the somewhat obvious conclusion that better prediction algorithms will ultimately lead to lower rated storage devices.

C. Transient Characteristics

The response of the system to faults was then tested to determine whether improvements in the transient response can

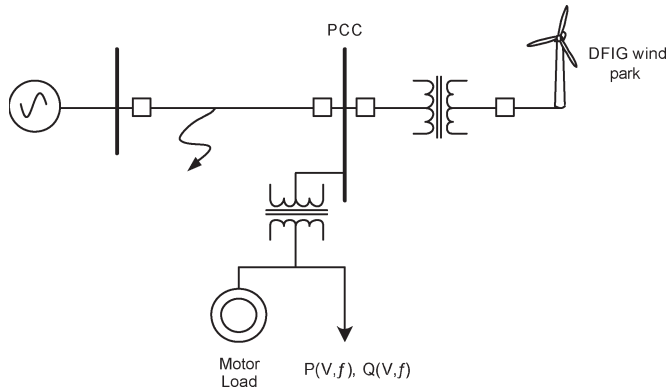


Fig. 8. Interconnection of wind and local load to a 69-kV transmission network used for transient characteristics studies (three-phase fault located at 1/5 the distance from the PCC).

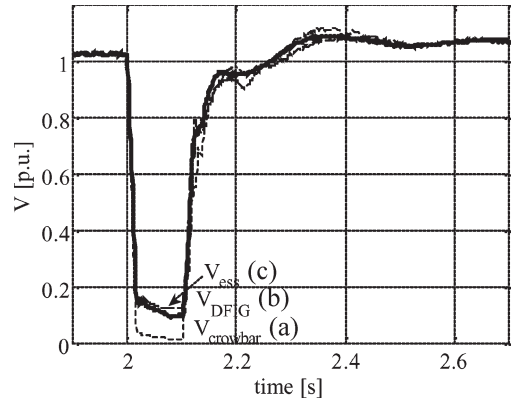


Fig. 9. Response of the voltage at the PCC following a three-phase six-cycle fault near the PCC for (a) DFIG with an active crowbar, (b) DFIG with derated converters, and (c) DFIG-ESS.

be achieved using storage. The system was first subjected to the most commonly occurring system faults—single-phase faults—however, as no noticeable differences were observed for different storage levels, the results are not presented here. Thus, more extreme contingencies were then considered. The test system in Fig. 8 was used, which consists of a small wind park connected to the 69-kV system, feeding a small local load with rotating machines, representing 50% of the total load.

Two types of serious contingencies were considered: a 12-cycle two-phase fault at the midpoint of the line and a six-cycle three-phase fault near the point of the common coupling (PCC). The response was obtained for the conventional DFIG, equipped with active crowbar, which is engaged for high rotor currents. A DFIG with overrated rotor-side converters capable of supporting the transient overcurrent was also considered to provide a picture of the influence of the crowbar. These two conventional DFIG ride-through topologies were compared with the DFIG-ESS, with a rating of 1.0 p.u.

The responses of the three topologies to the three-phase fault are presented here (Figs. 9 and 10). Similar trends appear in the case of two-phase faults, and therefore, they have not been included. The effect of the crowbar is most evident by looking at V_{pcc} —the internal voltage of the machine is lost because V_{pcc} drops to nearly zero, which is analogous to the response of an induction generator (Fig. 9). The DFIG-ESS and the DFIG that maintain control of the rotor-side voltages are both able to maintain the internal flux, which helps support the voltage at the PCC. The drop is somewhat less in the case of the DFIG-ESS due to the ability to firmly hold the dc voltage.

These results are corroborated when considering the reactive powers (Fig. 10). While $Q_{crowbar}$ goes to zero during the fault, both Q_{ess} and Q_{DFIG} are able to supply reactive power. Following fault clearing, the crowbar is disengaged, and reactive power can be supplied to help bring up the voltage. However, in the other two cases, the voltage has already started to recover due to the control action during the fault and settles faster to its pre-fault value.

The motivation here was to demonstrate the benefit of storage during transients; however, the importance of maintaining control over the machine during the fault appears to be an even

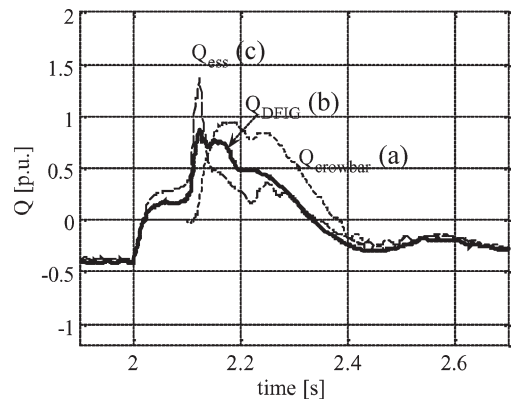


Fig. 10. Response of the reactive power following a three-phase six-cycle fault near the PCC for (a) DFIG with an active crowbar, (b) DFIG with derated converters, and (c) DFIG-ESS.

more crucial factor. That said, the ESS does provide a further improvement—one that will most certainly become more evident for longer fault durations, as are required by LVRT requirements.

V. CONCLUSION

This paper has evaluated the ability of an ESS to improve the performance of a DFIG-based wind generator. The impact of the capacity of the storage device, errors in estimated wind power, and different transient control strategies were investigated. Results show that for storage levels rated using the area above the LVRT curve, the output power can be effectively smoothed to the predicted hourly output power when the prediction is accurate. Errors in prediction will undeniably require larger rated storage devices to achieve the same level of performance. Although the storage management scheme is able to adjust to accommodate errors in wind power prediction, long-term storage would be required in order to continue to provide a preset power output. During transients, the storage device provides an effective means to ride through disturbances and exhibits superior characteristics during and following extreme voltage events.

APPENDIX

TABLE III
DATA USED FOR THE SIZING OF AN ESS IN A DFIG

P_{wind} (MW)	V_{dc} (V)	V_{min} (p.u.)	t_1 (s)	t_2 (s)
1	1200	0.15	0.625	3

TABLE IV
STORAGE SYSTEM CHARACTERISTICS SIZED USING LVRT

E_{LVRT} (MJ)	C_{ess} (F)	P_{ess} (MW)	$V_{ess,base}$ (V)	$I_{ess,base}$ (A)	$I_{ess,max}^i$ (p.u.)
1.66	2.31	0.5	1200	833	2.5

i – assumes operation at $P_{ess,rated}$ and $V_{ess,min} = 0.2$ p.u.

TABLE V
STATIC LOAD CHARACTERISTICS

V_o (kV)	P_o (MW)	f_o (Hz)	Q_o (MVAr)	a	b	c	d
6.6	4	60	1	1.3	3	1	2.8

TABLE VI
DYNAMIC LOAD CHARACTERISTICS

Machine Type	P_{rated} (MW)	pf ⁱ	V_{base} (kV)	poles	H (s)
Induction	3.73	0.906	6.6	4	1.3

i - 120 μ F capacitance connected in shunt to compensate motor load

TABLE VII
TRANSMISSION LINE PARAMETERS FOR THE TEST FEEDER

SCR	S_{base} (MVA)	R' (Ω /km)	L' (Ω /km)	C' (S/km)
6	10	0.53	1.59	5.21

ACKNOWLEDGMENT

The authors would like to thank the Natural Science and Engineering Research Council of Canada for their support of this research. Thanks are also extended to J. Restrepo for his editorial and formatting aid.

REFERENCES

- [1] C. Jauch, J. Matevosyan, T. Ackermann, and S. Bolik, "International comparison of requirements for connection of wind turbines to power systems," *Wind Energy*, vol. 8, no. 3, pp. 295–306, Jul./Sep. 2005.
- [2] J. W. Smith, J. A. Taylor, D. L. Brooks, and R. C. Dugan, "Interconnection studies for wind generation," in *Proc. Rural Elect. Power Conf.*, May 2004, pp. C3-1–C3-8.

- [3] E. Bossanyi, Z. Saad-Saoud, and N. Jenkins, "Prediction of flicker produced by wind turbines," *Wind Energy*, vol. 1, no. 1, pp. 35–51, 1998.
- [4] J. H. R. Enslin, J. Krijp, C. P. J. Jansen, and P. Bauer, "Integrated approach to network stability and wind energy technology for on-shore and offshore applications," in *Proc. Power Quality*, May 2003, pp. 185–192.
- [5] L. Ran, J. R. Bumby, and P. J. Tavner, "Use of turbine inertia for power smoothing of wind turbines with a DFIG," in *Proc. 11th Int. Conf. Harmonics and Quality Power*, Sep. 2004, pp. 106–111.
- [6] K. Strunz and E. K. Brock, "Hybrid plant of renewable stochastic source and multilevel storage for emission-free deterministic power generation," in *Proc. Quality and Security Elect. Power Delivery Syst., CIGRE/IEEE PES Int. Symp.*, Oct. 8–10, 2003, pp. 214–218.
- [7] J. P. Barton and D. G. Infield, "Energy storage and its use with intermittent renewable energy," *IEEE Trans. Energy Convers.*, vol. 19, no. 2, pp. 441–448, Jun. 2004.
- [8] R. Cardenas, R. Pena, G. Asher, and J. Clare, "Power smoothing in wind generation systems using a sensorless vector controlled induction machine driving a flywheel," *IEEE Trans. Energy Convers.*, vol. 19, no. 1, pp. 206–216, Mar. 2004.
- [9] E. ON Netz GmbH, *Grid Code for High and Extra High Voltage*, Aug. 2003, Bayreuth, Germany. [Online]. Available: www.eon-netz.com
- [10] S. Buller, E. Karden, D. Kok, and R. W. De Doncker, "Modeling the dynamic behavior of supercapacitors using impedance spectroscopy," *IEEE Trans. Ind. Appl.*, vol. 38, no. 6, pp. 1622–1626, Nov./Dec. 2002.
- [11] C. Abbey and G. Joos, "A doubly-fed induction machine and energy storage system for wind power applications," in *Proc. IEEE PESC*, Aachen, Germany, Jun. 20–25, 2004, vol. 3, pp. 1964–1968.
- [12] A. B. Marques, G. N. Taranto, and D. M. Falcao, "A knowledge-based system for supervision and control of regional voltage profile and security," *IEEE Trans. Power Syst.*, vol. 20, no. 1, pp. 400–407, Feb. 2005.



Chad Abbey (S'01) received the B.Sc. degree in electrical engineering from the University of Alberta, Edmonton, AB, Canada, in 2002, and the M.Eng. degree in electrical engineering from McGill University, Montréal, QC, Canada, in 2004, where he is currently working toward the Ph.D. degree.

He is currently with the CANMET Energy Technology Centre, Varennes, QC, as a Research Engineer, where he helps in coordinating a joint research program on the modeling and integration of distributed generation. His current research interests

include wind energy, distributed generation, energy storage, and their integration to the grid.

Mr. Abbey is an active member of the International Council on Large Electric Systems (CIGRE).



Géza Joos (M'82–SM'89–F'06) received the M.Eng. and Ph.D. degrees from McGill University, Montréal, QC, Canada.

He has been with McGill University as a Professor since 2001. He is involved in fundamental and applied research related to the application of high-power electronics to power conversion, including distributed generation, and power systems. He was also with ABB, the University of Quebec, Sainte Foy, QC, and Concordia University, Montréal. He has been involved in consulting activities in Power

Electronics and Power Systems, and with CEA Technologies as the Technology Coordinator of the Power Systems Planning and Operations Interest Group. He has published extensively and presented numerous papers and tutorials on these topics.

Dr. Joos is a Fellow of the Canadian Academy of Engineering. He is active in a number of IEEE Industry Applications Society committees and in IEEE Power Engineering Society and International Council on Large Electric Systems (CIGRE) activities and working groups that deal with power electronics and applications to distributed resources.